Pakistan Veterinary Journal

ISSN: 0253-8318 (PRINT), 2074-7764 (ONLINE)
DOI: 10.29261/pakvetj/2026.236

RESEARCH ARTICLE

Genetic Diversity, Antimicrobial Resistance, and Pathogenic Potential of Pulmonary *Escherichia coli* Isolates from Forest Musk Deer with Fatal Hemorrhagic Pneumonia

Wei Dou[1], Fan Yang[3], Shutong Feng[1], Yuxin Fan[1], Wenhui Liu[4], Yi Jiang[1], Muhammad Taimoor[5,6], Yiwei Yuan[1], Liangyi Zhang[1], Zhongyuan Ma[1], Rongjie Yan[3], Xiaobin Zhao[3], Changrong Lv[1*], Liang Zhang[1*] and Kangkang Guo[1,2*]

[1]College of Veterinary Medicine, Northwest A&F University, Yangling, Shaanxi 712100, China; [2]College of Animal Science and Technology, Xizang Vocational Technical College, Lhasa, Xizang 850000, China; [3]Ecological and Wildlife Conservation Management Station, Baoji, Shaanxi 721703, China; [4]Zhangzhou Health Vocational College, Zhangzhou, Fujian 363000, China; [5]Department of Pathobiology, Riphah College of Veterinary Sciences (RCVetS), Riphah International University, Lahore Campus, Lahore 54000, Pakistan; [6]Research & Development Division, Veterinary Research Institute, Lahore 54810, Pakistan
*Corresponding author: guokk2007@nwsuaf.edu.cn (KG); eerduosizl@163.com (LZ); 447009924@qq.com (CL)

ARTICLE HISTORY (26-776)

Received: June 26, 2026
Revised: August 20, 2026
Accepted: August 22, 2026
Published online: October 22, 2026

Key words:
Antimicrobial resistance
Escherichia coli
Forest musk deer
Hemorrhagic pneumonia

ABSTRACT

Forest musk deer (*Moschus berezovskii*) is an endangered species with high medicinal value. Hemorrhagic pneumonia, characterized by acute onset and high mortality, frequently occurs in captive forest musk deer, seriously restricting captive breeding. However, its etiological agents and pathogenesis remain unclear. In this study, 43 lung tissue samples were collected from forest musk deer that died of hemorrhagic pneumonia between 2023 and 2025. Exploratory metatranscriptomic analysis of 3 selected samples indicated bacterial predominance, with several opportunistic pathogens, including *Escherichia coli* (*E. coli*), *Pasteurella multocida (P. multocida)*, and *Acinetobacter baumannii (A. baumannii)*, showing relatively high abundance. Bacterial isolation identified *E. coli* as the most frequent species (39/89; 43.82%). The isolates exhibited resistance to multiple commonly used antimicrobials; ampicillin (AMP) resistance exceeded 50% in each year. Multilocus sequence typing (MLST) identified 16 assigned sequence types (STs), including ST357, ST224, and ST95, as well as 4 unassigned profiles among the 39 isolates. Representative isolates induced hemorrhagic lung lesions in mice. These findings indicate an association between *E. coli* and hemorrhagic pneumonia in forest musk deer, providing a basis for disease surveillance and control.

To Cite This Article: Dou W, Yang F, Feng S, Fan Y, Liu W, Jiang Y, Taimoor M, Yuan Y, Zhang L, Ma Z, Yan R, Zhao X, Lv C, Zhang L and Guo K, 2026. Genetic diversity, antimicrobial resistance, and pathogenic potential of pulmonary *Escherichia coli* isolates from forest musk deer with fatal hemorrhagic pneumonia. Pak Vet J, 46(10): 2540-2551. http://dx.doi.org/10.29261/pakvetj/2026.236

INTRODUCTION

Forest musk deer (*Moschus berezovskii*) is an endangered artiodactyl species. Musk produced by adult males is highly valued in traditional Chinese medicine and perfume production (Fan *et al.*, 2019). Since the 1950s, the medicinal and cultural value of musk has exposed this species to multiple threats, including poaching and habitat destruction, bringing wild populations to the brink of extinction (Liu *et al.*, 2024; Yi *et al.*, 2025). To protect and restore forest musk deer populations, captive breeding programs for this species were initiated in China in 1958, and captive populations have since been established in various regions, mainly Shaanxi and Sichuan (Jiang *et al.*, 2022).

With the gradual expansion of captive breeding programs, diseases have become increasingly prevalent, severely constraining sustainable captive breeding (Wang *et al.*, 2023). One such critical illness is hemorrhagic pneumonia, which is a major respiratory disease in captive forest musk deer, characterized by rapid progression, high mortality, and inconspicuous early clinical signs (Qi *et al.*, 2024; Deng *et al.*, 2025). Antibiotic therapy is the primary treatment for this disease. However, prolonged use of antibiotics may promote antibiotic resistance and compromise treatment efficacy (Chen *et al.*, 2022). Therefore, elucidating the major etiological agents and pathogenic mechanisms of hemorrhagic pneumonia is essential for effective prevention and control.

Hemorrhagic pneumonia has a complex etiological spectrum and may result from single or mixed infections involving diverse pathogens, including bacteria, viruses, mycoplasmas, and fungi (Lubkin *et al.*, 2024). Common bacterial pathogens associated with hemorrhagic pneumonia include *Escherichia coli* (*E. coli*), *Klebsiella pneumoniae (K. pneumoniae)*, *Pseudomonas aeruginosa (P. aeruginosa)*, and *Pasteurella multocida (P. multocida)* (Wan *et al.*, 2025). This disease is likely to occur in captive environments characterized by high stocking densities and multiple stressors (Zhou *et al.*, 2023). In cases of hemorrhagic pneumonia across different animal species, colonization and invasion by opportunistic pathogens are considered critical steps in disease development and progression. However, predominant pathogens may vary substantially depending on the host species and environmental conditions (Huang *et al.*, 2019; Miao *et al.*, 2023). As an opportunistic pathogen with strong adaptability and diverse pathogenic potential, *E. coli* is widely distributed in nature. When host immune function is impaired or intestinal microbial homeostasis is disrupted, *E. coli* may shift from a commensal bacterium to an opportunistic pathogen. It may also invade extraintestinal tissues and organs through wounds, the respiratory tract, or the bloodstream, thereby causing various infectious diseases (Kobayashi *et al.*, 2021).

E. coli can cause both enteric and extraintestinal disease, including diarrhea, enteritis, pneumonia, septicemia, urinary tract infection, and peritonitis, thereby posing substantial health challenges in humans and animals. *E. coli* is associated with respiratory diseases in various animals, including ostriches, broiler chickens, goats, and dogs (Coe *et al.*, 2022; Yun *et al.*, 2022; Yehia *et al.*, 2023; Iorgoni *et al.*, 2025). Several potential pathogens, including *P. aeruginosa*, *E. coli*, and *K. pneumoniae*, have been isolated from the lung tissues of forest musk deer with hemorrhagic pneumonia (Zhao *et al.*, 2017; Yang *et al.*, 2020; Zhao *et al.*, 2020; Lu *et al.*, 2022; Zhang *et al.*, 2024); however, systematic investigations of the associated pathogens, pulmonary microbial community structure, and pathogenic characteristics remain limited.

Despite the increasing prevalence of hemorrhagic pneumonia in captive forest musk deer and its severe impact on breeding sustainability, the predominant etiological agents and pathogenic characteristics of this disease remain poorly defined. This knowledge gap limits the development of targeted diagnostic, surveillance, and treatment strategies for this disease in captive forest musk deer. Therefore, this study investigated bacterial pathogens associated with fatal hemorrhagic pneumonia in captive forest musk deer using metatranscriptomic sequencing, bacterial isolation, antimicrobial susceptibility testing, phylogenetic analysis, and multilocus sequence typing (MLST) of lung samples collected from deceased animals in Shaanxi Province, China.

MATERIALS AND METHODS

Sample collection: From September 2023 to December 2025, 43 lung samples from forest musk deer that died of hemorrhagic pneumonia and 10 lung samples from forest musk deer that died of non-hemorrhagic pneumonia were aseptically collected from 40 captive farms in Shaanxi Province, China. Necropsy and sampling were performed within 2h of death. Tissues from deep pulmonary lesions were transported on ice and cultured within 6h; samples for metatranscriptomic sequencing were stored at -80°C.

Metatranscriptomic sequencing and viral screening: Three samples (F1–F3) were randomly selected from 43 uniquely numbered lung samples using a Python-generated sequence. After RNA extraction and ribosomal RNA (rRNA) depletion, 150-bp paired-end libraries were sequenced on an Illumina NovaSeq 6000 (Novogene, Beijing, China). Reads were quality-filtered using fastp, host-derived reads were removed by alignment to the reference genome, and non-host reads were assembled with Trinity, dereplicated with CORSET (0.95), annotated against the National Center for Biotechnology Information (NCBI) non-redundant (NR) database using DIAMOND (E-value $\leq 1\times10^{-5}$), and classified with MEGAN. Samples with virus-related reads underwent virus isolation in Vero cells and PCR confirmation, followed by Sanger sequencing and BLASTn analysis.

Bacterial isolation, identification, and phylogenetic analysis: Lesion tissues were cultured on blood agar at 37°C for 18–24h. One well-isolated colony representing each distinct morphotype was purified and identified by *16S rRNA* gene sequencing using primers 27F (5'-AGAGTTTGATCCTGGCTCAG-3') and 1492R (5'-TACGGCTACCTTGTTACGACTT-3'); when multiple colonies showed the same morphology, only one was selected. One confirmed *E. coli* isolate was retained from each *E. coli*-positive lung for subsequent analyses. Sequences were compared with GenBank using BLASTn, and isolates showing ≥99% identity to *E. coli* were retained. A maximum-likelihood tree based on *16S rRNA* gene sequences was constructed in MEGA7 using the Kimura two-parameter model with 1,000 bootstrap replicates.

Antimicrobial susceptibility testing: Kirby–Bauer disk diffusion was performed on Mueller–Hinton agar using 0.5 McFarland suspensions, and the inoculated plates were incubated at 37°C for 16h. Interpretive categories and zone-diameter breakpoints for disk diffusion were based on the M100 standard of the Clinical and Laboratory Standards Institute (CLSI, 2023) and the product information provided by Hangzhou Microbial Reagent Co., Ltd. (Hangzhou, China). Resistance rates were calculated as the proportion of resistant isolates, with intermediate isolates not classified as resistant. Multidrug resistance (MDR) was defined as acquired non-susceptibility to ≥1 agent in ≥3 antimicrobial categories, with intermediate and resistant phenotypes considered non-susceptible. *E. coli* ATCC 25922 served as the quality-control strain.

MLST and virulence gene detection: Seven-locus Achtman MLST was performed using primers in Table 1. Allelic profiles and sequence types (STs) were assigned by comparison with the PubMLST database. Twelve *E. coli*

virulence-associated genes linked to extraintestinal pathogenicity were screened by PCR using primers in Table 2.

Table 1: Primers for housekeeping genes.

Primer	Sequences (5'-3')	Product size (bp)	Annealing Temperature (°C)
adk	F: TCATCATCTGCACTTTCCGC R: CCAGATCAGCGCGAACTTCA	583	54
fumC	F: TCACAGGTCGCCAGCGCTTC R: GTACGCAGCGAAAAAGATTC	806	54
gyrB	F: TCGGCGACACGGATGACGGC R: ATCAGGCCTTCACGCGCATC	911	57
icd	F: ATGGAAAGTAAAGTAGTTGTTCCGGCACA R: GGACGCAGCAGGATCTGTT	878	55
mdh	F: ATGAAAGTCGCAGTCCTCGGCGCTGCTGGCGG R: TTAACGAACTCCTGCCCCAGAGCGATATCTTTCTT	932	57
purA	F: TCGGTAACGGTGTTGTGCTG R: CATACGGTAAGCCACGCAGA	816	54
recA	F: CGCATTCGCTTTACCCTGACC R: TCGTCGAAATCTACGGACCGGA	780	54

Table 2: Primers for virulence genes.

Primer	Sequences (5'-3')	Product size (bp)	Annealing Temperature (°C)
fimH	F: TGCAGAACGGATAAGCCGTGG R: GCAGTCACCTGCCCTCCGGTA	508	57
fimC	F: GGGTAGAAAATGCCGATGGTG R: CGTAATTTTGGGGGTAAGTGC	497	57
iroN	F: AAGTCAAAGCAGGGGTTGCCCG R: GACGCCGACATTAAGACGCAG	667	63
iutA	F: GGCTGGACATCATGGGAACTGG R: CGTCGGGAACGGGTAGAATCG	302	61
kpsMTII	F: GCGCATTTGCTGATACTGTTG R: CATCCAGACGATAAGCATGAGCA	272	55
hlyA	F: AACAAGGATAAGCACTGTTCTGGCT R: ACCATATAAGCGGTCATTCCCGTCA	1177	58
hlyF	F: GGCGATTTAGGCATTCCGATACTC R: ACGGGGTCGCTAGTTAAGGAG	599	57
cnf1	F: AAGATGGAGTTTCCTATGCAGGAG R: CATTCAGAGTCCTGCCCTCATTATT	498	61
papC	F: GACGGCTGTACTGCAGGGTGTGGCG R: ATATCCTTTCTGCAGGGATGCAATA	328	58
sfaS	F: GTCTCTCACCGGATGCCAGAATAT R: GCATTACTTCCATCCCTGTCCTG	138	55
focD	F: CGGAGGAGTAATTACAAACCTGGCA R: CTCCGGAGAACTGGGTGCATCTTAC	410	55
irp2	F: AAGGATTCGCTGTTACCGGAC R: TCGTCGGGCAGCGTTTCTTCT	264	55

Mouse pathogenicity assay: Twenty-four specific-pathogen-free (SPF) Kunming mice (18-22g; equal numbers of males and females) were randomly assigned to three infection groups and one control group (n=6/group). *E. coli* 02, *E. coli* 20 and *E. coli* 32, representing the three most prevalent STs, were cultured in Luria-Bertani (LB) broth for 12h and adjusted to 1×10^{8}cfu/mL. Mice were inoculated intraperitoneally with 0.2mL of each suspension; controls received sterile LB broth. Clinical signs and mortality were recorded for 36h. No predefined humane endpoints were specified. Dead mice were necropsied immediately, and survivors were euthanized by cervical dislocation at the end of the observation period by trained personnel. Organ bacterial loads were determined by plate counting, and bacteria were re-isolated from deep lung tissues on blood agar and LB agar and identified by *16S rRNA* sequencing and MLST. Lung tissues were fixed in 4% paraformaldehyde, paraffin-embedded, sectioned, Hematoxylin & Eosin (H&E) stained, and examined microscopically.

Statistical analysis: Annual proportions and pairwise survival comparisons were analyzed in R 4.5.3, and correlation and overall survival analyses in GraphPad Prism 8.0. Annual resistance rates, MDR proportions, and virulence-gene frequencies were compared using the Fisher-Freeman-Halton exact test, with 95% CIs calculated by the Wilson method. *P* values for antimicrobial-agent and virulence-gene comparisons were adjusted separately by Holm's method. Spearman's rank correlation assessed the association between virulence-gene number and the number of antimicrobial agents resisted. Survival among the four groups was compared using the log-rank test, with 36h survivors right-censored. Post-hoc pairwise log-rank comparisons were performed among the four groups, with *P* values adjusted using Holm's method. Two-sided $P<0.05$ was considered significant.

RESULTS

Metatranscriptomic profiling and viral validation: Exploratory metatranscriptomic profiling of F1–F3 showed that bacteria dominated the microbial communities, accounting for 58, 67 and 62% of the total reads, respectively (Fig. 1A). At the species level, F2 and F3 clustered together, whereas F1 formed a separate branch. Several bacterial taxa, including *K. pneumoniae*, *Enterococcus faecium (E. faecium)*, *E. coli*, *P. multocida*, *Enterococcus faecalis (E. faecalis)* and *Acinetobacter baumannii (A. baumannii)*, were relatively abundant. Virus-related reads assigned to feline leukemia virus, Orf virus and avian leukosis virus were also detected (Fig. 1B). However, no viruses were isolated. Although PCR of lung tissues yielded bands of the expected size, BLAST analysis of the amplicons showed greater similarity to forest musk deer genomic sequences, suggesting likely false-positive viral assignments.

Bacterial isolation from the lung tissues: Based on the high-throughput sequencing results, bacterial isolation and identification were performed on all 43 lung tissue samples collected from forest musk deer that died of hemorrhagic pneumonia. In total, 89 bacterial isolates belonging to 15 species, including *E. coli*, *P. aeruginosa*, *E. faecium*, *E. faecalis*, *Bacillus cereus* (*B. cereus*), and *Staphylococcus haemolyticus* (*S. haemolyticus*), were recovered from these samples. From 2023 to 2025, *E. coli* was recovered from 12/13, 12/14, and 15/16 lung tissue samples, corresponding to isolation rates of 92.31, 85.71, and 93.75%, respectively. Overall, 39 *E. coli* isolates were obtained (Fig. 2A), accounting for 43.82% of the bacterial isolates. *E. faecalis*, *E. faecium*, and *Raoultella ornithinolytica* (*R. ornithinolytica*) were also isolated at rates of 10.11, 8.99, and 6.74%, respectively, whereas the isolation rates of the remaining bacterial taxa were all below 5% (Fig. 2B). In contrast, *E. coli* was not isolated from any of the 10 lung tissue samples collected from forest musk deer that died of non-hemorrhagic pneumonia (Fig. 2C). In each of the three study years, *E. coli* was isolated from more than 85% of lung samples from forest musk deer with hemorrhagic pneumonia (Fig. 2D).

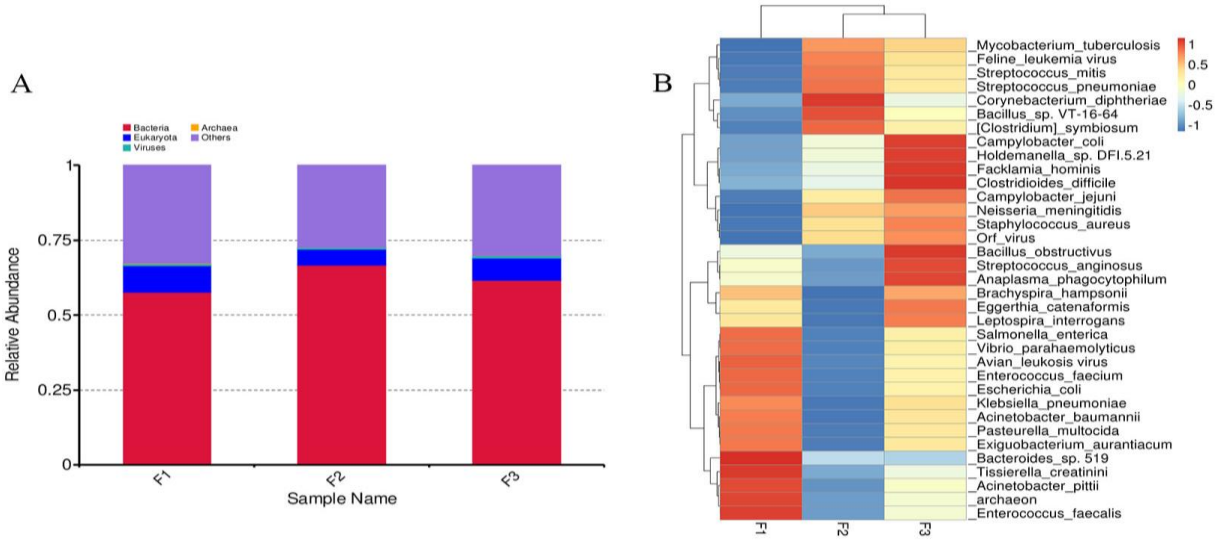


Fig. 1: Microbial composition of lung tissues. (A) Kingdom-level relative abundances. (B) Abundance clustering heatmap of the top 35 microbial species.

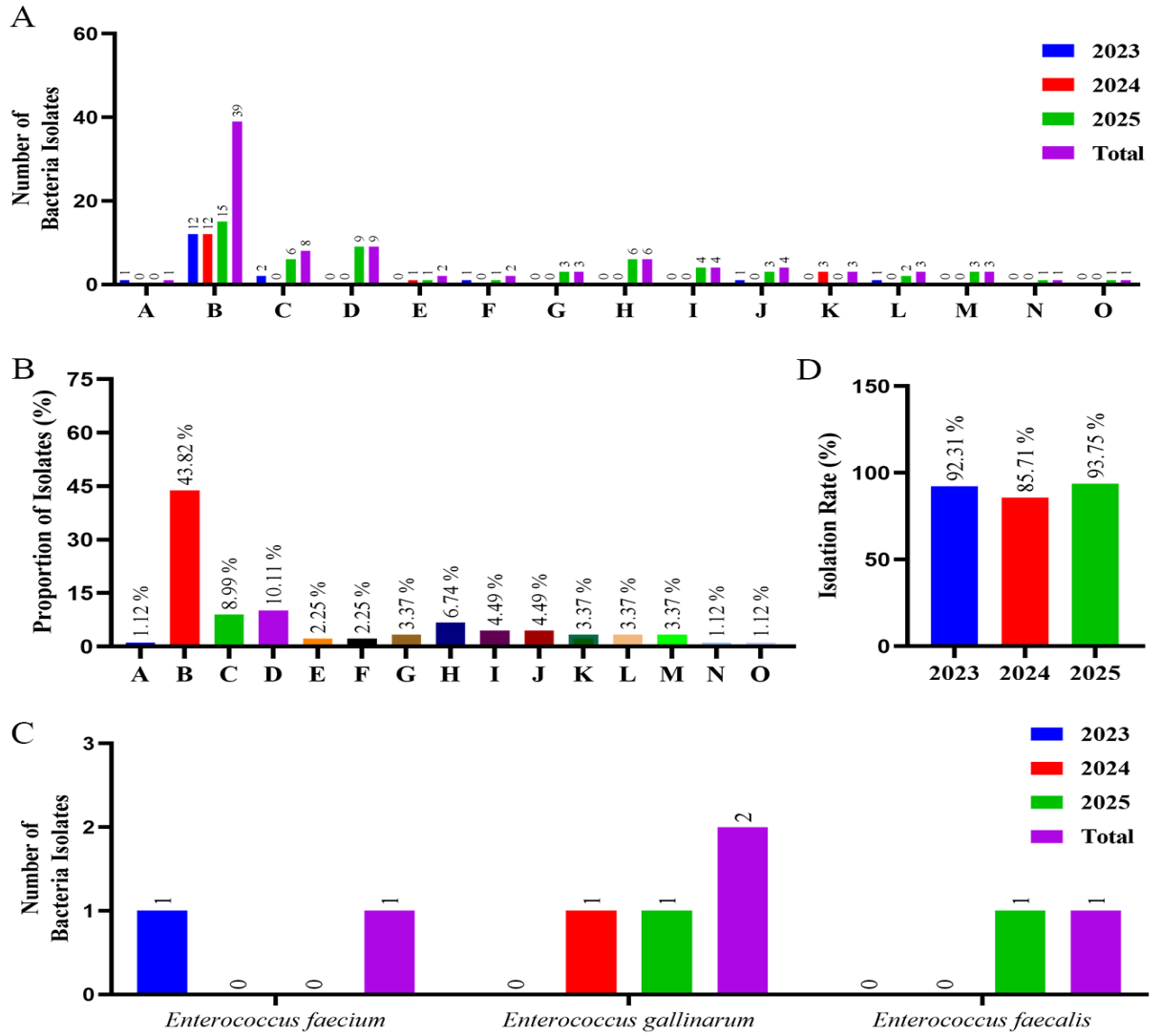


Fig. 2: Bacterial isolation results and distribution of *E. coli* across lung tissue samples. (A) Numbers of bacterial isolates from lung tissues of forest musk deer that died of hemorrhagic pneumonia, (B) Proportions of bacterial isolates from lung tissues of forest musk deer that died of hemorrhagic pneumonia, (C) Numbers of bacterial isolates from lung tissues of forest musk deer that died of non-hemorrhagic pneumonia, (D) Annual *E. coli* isolation rates from lung tissues of forest musk deer that died of hemorrhagic pneumonia. In panels A and B, A–O denote bacterial species: A. *Pseudomonas aeruginosa*, B. *E. coli*, C. *Enterococcus faecium*, D. *Enterococcus faecalis*, E. *Bacillus licheniformis*, F. *Bacillus subtilis*, G. *Bacillus cereus*, H. *Raoultella ornithinolytica*, I. *Enterococcus gallinarum*, J. *Enterobacter hormaechei*, K. *Streptococcus gallolyticus*, L. *Acinetobacter baumannii*, M. *Hafnia alvei*, N. *Klebsiella pneumoniae*, O. *Staphylococcus haemolyticus*.

Phylogenetic analysis of pulmonary *E. coli* isolates based on *16S rRNA* gene sequences: The 39 *E. coli* isolates were distributed across multiple branches of the *16S rRNA*-based phylogenetic tree. Isolates obtained in 2023-2025 were interspersed throughout the tree, with no clear year-specific clustering. Reference strains from humans, pigs, cattle, sheep, goats, poultry, forest musk deer, and soil were distributed among different branches. Several forest musk deer-derived *E. coli* isolates clustered with reference strains from soil, avian, goat, and human sources. For example, *E. coli* 17 clustered with soil- and avian-derived strains, whereas *E. coli* 09 grouped with goat- and human-derived strains. Twelve isolates formed a distinct branch with the avian-derived strain CP011915.1, while the remaining isolates were distributed across several sublineages (Fig. 3).

Antimicrobial resistance profiles of *E. coli* isolates: All 39 *E. coli* isolates were tested against 10 antimicrobial agents, and 31 isolates were resistant to at least one agent (Fig. 4A). In 2023, the highest resistance rates were observed for ampicillin (AMP) (66.67%; 8/12) and streptomycin (STR) (50.00%; 6/12). In 2024, AMP and ciprofloxacin (CIP) showed the highest resistance rates (75.00%; 9/12 each), followed by STR (66.67%; 8/12). In 2025, the highest resistance rates were observed for AMP and STR (80.00%; 12/15 each), followed by CIP (66.67%; 10/15) and gentamicin (GEN) (60.00%; 9/15) (Fig. 4B). No significant differences in resistance rates were detected among different years for the antimicrobial agents tested after Holm adjustment (all $P>0.05$). The proportions of MDR isolates were 58.33 (7/12), 75.00 (9/12), and 73.33% (11/15) in 2023, 2024, and 2025, respectively (Fig. 4C), with no significant difference among years ($P=0.685$).

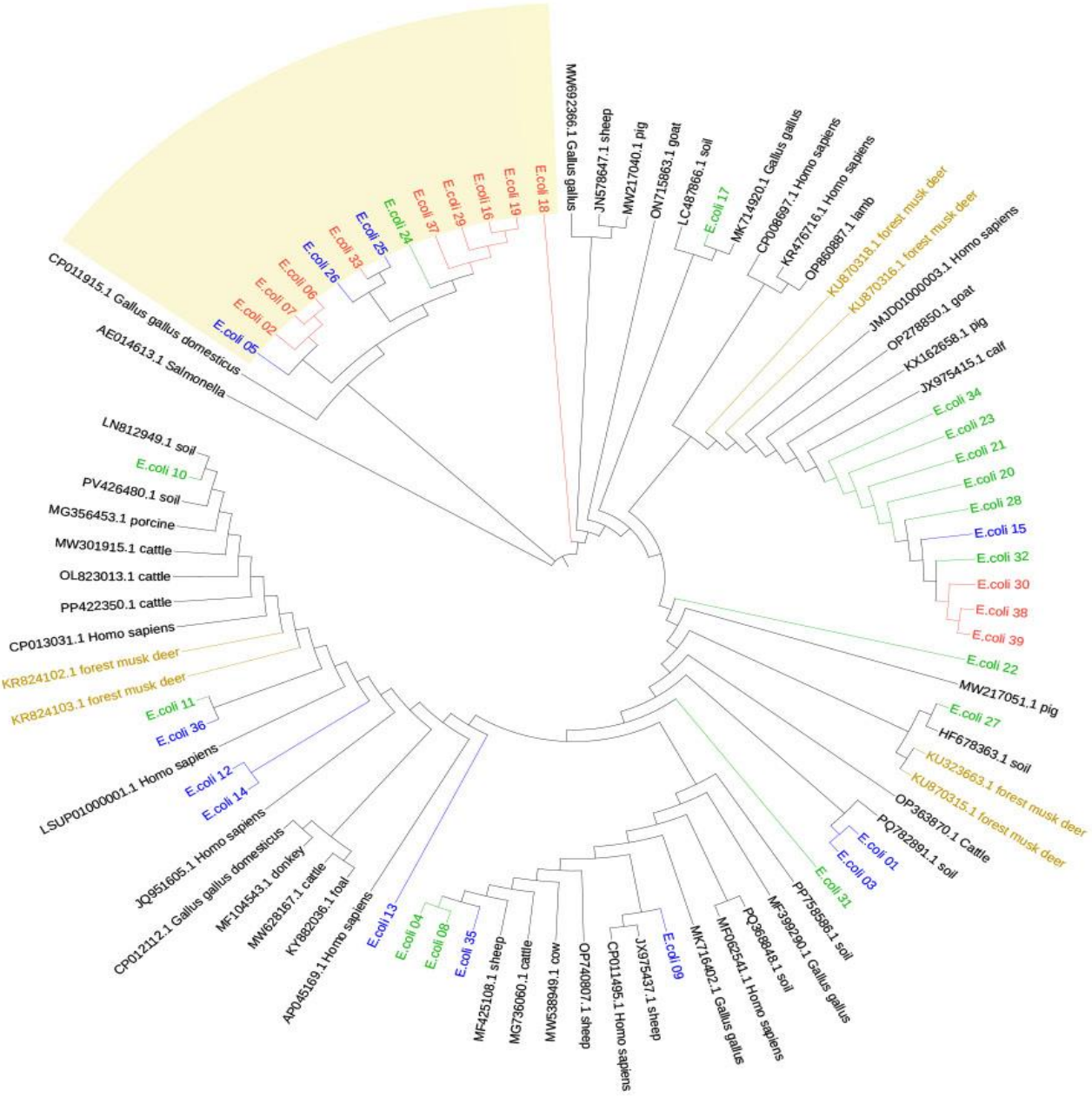


Fig. 3: Maximum-likelihood phylogenetic analysis of 39 pulmonary *E. coli* isolates from forest musk deer and reference isolates from diverse sources. 2023, 2024, 2025, and known forest musk deer isolates are highlighted in blue, red, green, and yellow, respectively.

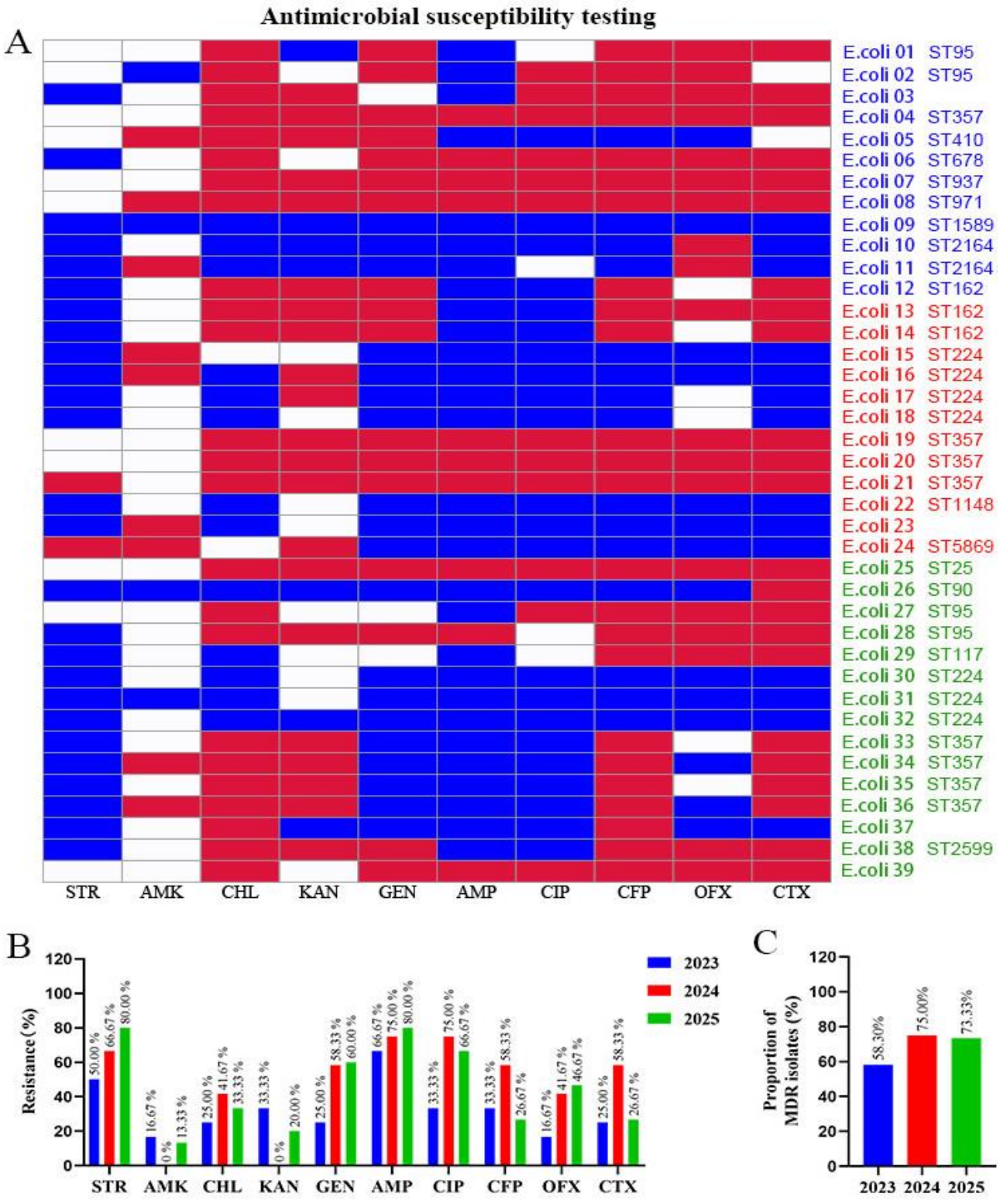


Fig. 4: Antimicrobial resistance profiles of *E. coli* isolates. (A) Heatmap of susceptibility to 10 antimicrobial agents. Labels indicate isolate and MLST designation. Red, white, and blue boxes indicate susceptible, intermediate, and resistant isolates, respectively. (B) Antimicrobial resistance rates of isolates from 2023 to 2025. (C) MDR rates of isolates from 2023 to 2025. STR, streptomycin; AMK, amikacin; CHL, chloramphenicol; KAN, kanamycin; GEN, gentamicin; AMP, ampicillin; CIP, ciprofloxacin; CFP, cefoperazone; OFX, ofloxacin; CTX, cefotaxime.

Molecular typing of *E. coli* isolates: Analysis of the 7 MLST housekeeping genes identified 72 alleles, including 2 novel alleles. The highest allelic diversity was observed for *fumC*, *gyrB*, *icd*, and *purA* (11 alleles each), whereas *adk* and *mdh* showed the lowest diversity (9 alleles each). Based on the seven-locus allelic profiles, the 39 isolates comprised 16 assigned STs and four unassigned profiles. ST357 was the most prevalent type (20.51%; 8/39), followed by ST224 (17.95%; 7/39) and ST95 (10.26%; 4/39) (Table 3).

Analysis of virulence gene carriage among *E. coli* isolates: A panel of 12 virulence-associated genes was screened among the forest musk deer-derived *E. coli*

isolates (Fig. 5A). *fimH* and *fimC* were detected in all isolates. Among the remaining genes, *irp2* showed the highest detection rate in 2023 and 2024 (50.00% each), whereas *hlyF* was most frequently detected in 2025 (33.33%), followed by *iutA* (26.67%) (Fig. 5B). Two-gene profiles were the most common in 2023, 2024, and 2025, accounting for 33.33 (4/12), 41.67 (5/12), and 60.00% (9/15), respectively. No significant differences in annual detection frequencies were found for any of the 12 virulence-associated genes after Holm adjustment (all $P>0.05$).

Comparison among isolates showed differences in virulence-gene and antimicrobial resistance profiles across several STs. All ST95 isolates had the same virulence-gene profile and were resistant to 1-2 antimicrobial agents, whereas all ST224 isolates carried only *fimH* and *fimC* and were resistant to 7-9 agents. All ST162 isolates had the same 6-gene profile and STR-AMP-CIP resistance phenotype. ST357 isolates obtained in 2023 and 2024 carried five genes and showed no phenotypic resistance to the tested antimicrobial agents, whereas those from 2025 carried only *fimH* and *fimC* and were resistant to 4-5 agents (Fig. 4A and 5A). Statistical analysis revealed a negative correlation between the number of virulence-associated genes and the number of antimicrobial agents to which the isolates were resistant (Spearman's $\rho=-0.498$, $P=0.001$).

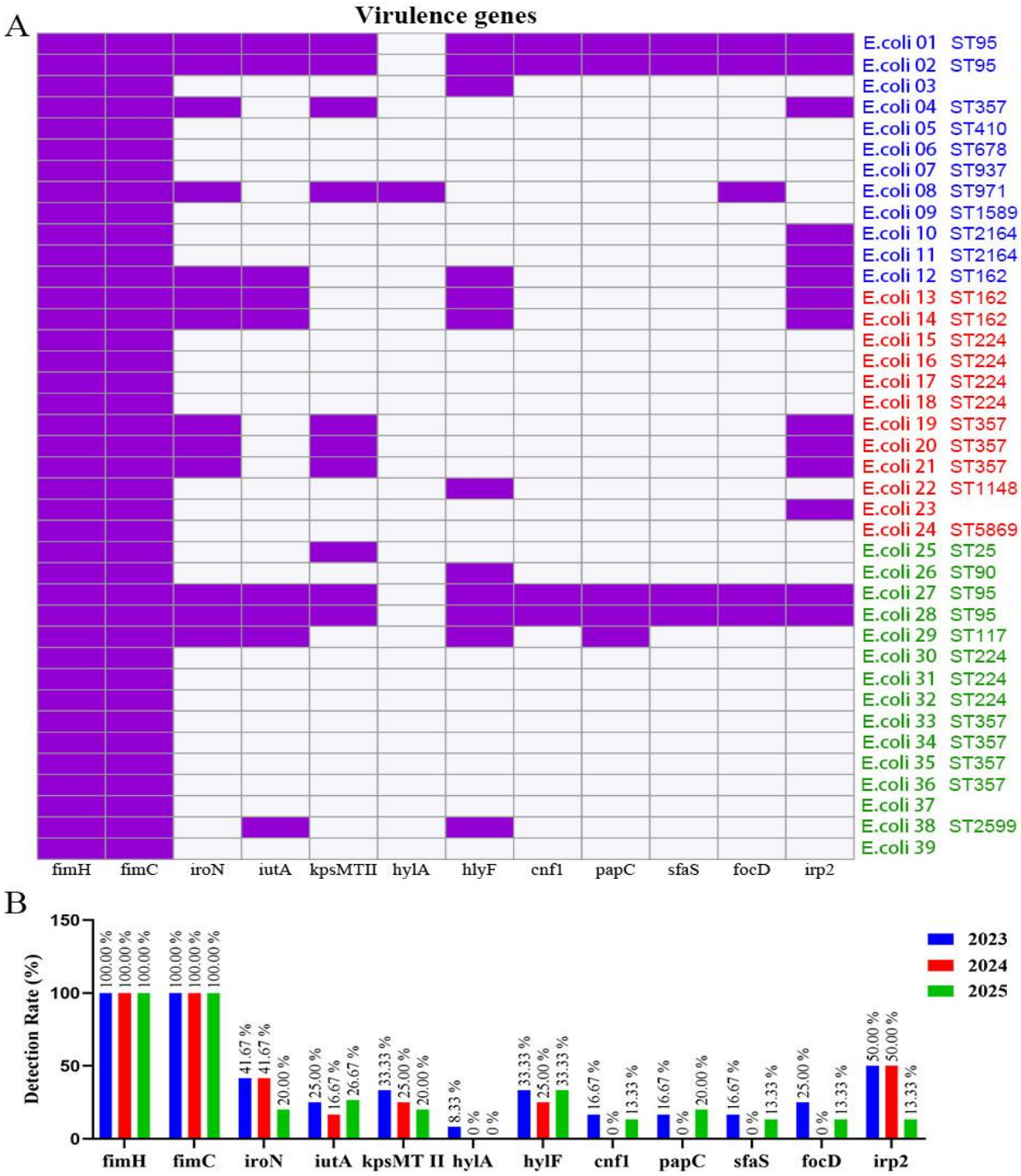


Fig. 5: Virulence gene profiles of *E. coli* isolates. **(A)** Heatmap of virulence-gene carriage. Labels indicate isolate and MLST designation. Purple and white boxes indicate gene presence and absence, respectively. **(B)** Annual detection rates of virulence genes from 2023 to 2025.

Pathogenicity of *E. coli* isolates in mice: All three selected *E. coli* isolates caused mortality in mice. *E. coli* 02 (ST95), 20 (ST357), and 32 (ST224) carried 11, 5, and 2 virulence-associated genes, respectively. Under the same challenge dose, all mice challenged with isolates 02 and 20 died within 12h and 17h, respectively, whereas 3 of 6 mice challenged with isolate 32 died within 24h and the remaining mice survived; no mortality occurred in the negative control group (Fig. 6A-D). Overall survival differed significantly among the four groups of mice (P<0.0001). Post-hoc pairwise log-rank comparisons showed significant differences among all three challenge groups and between the *E. coli* 02 and control groups and between the *E. coli* 20 and control groups (Holm-adjusted P = 0.0055 for all comparisons), whereas *E. coli* 32 did not differ significantly from the control (Holm-adjusted P = 0.0555). In mice challenged with *E. coli* 32, bacterial loads were highest in the intestine, followed by the spleen, liver, lung, kidney, and heart (Fig. 6E). *E. coli* was re-isolated from the lungs of challenged mice and identified as the corresponding challenge strains (Fig. 6F-G).

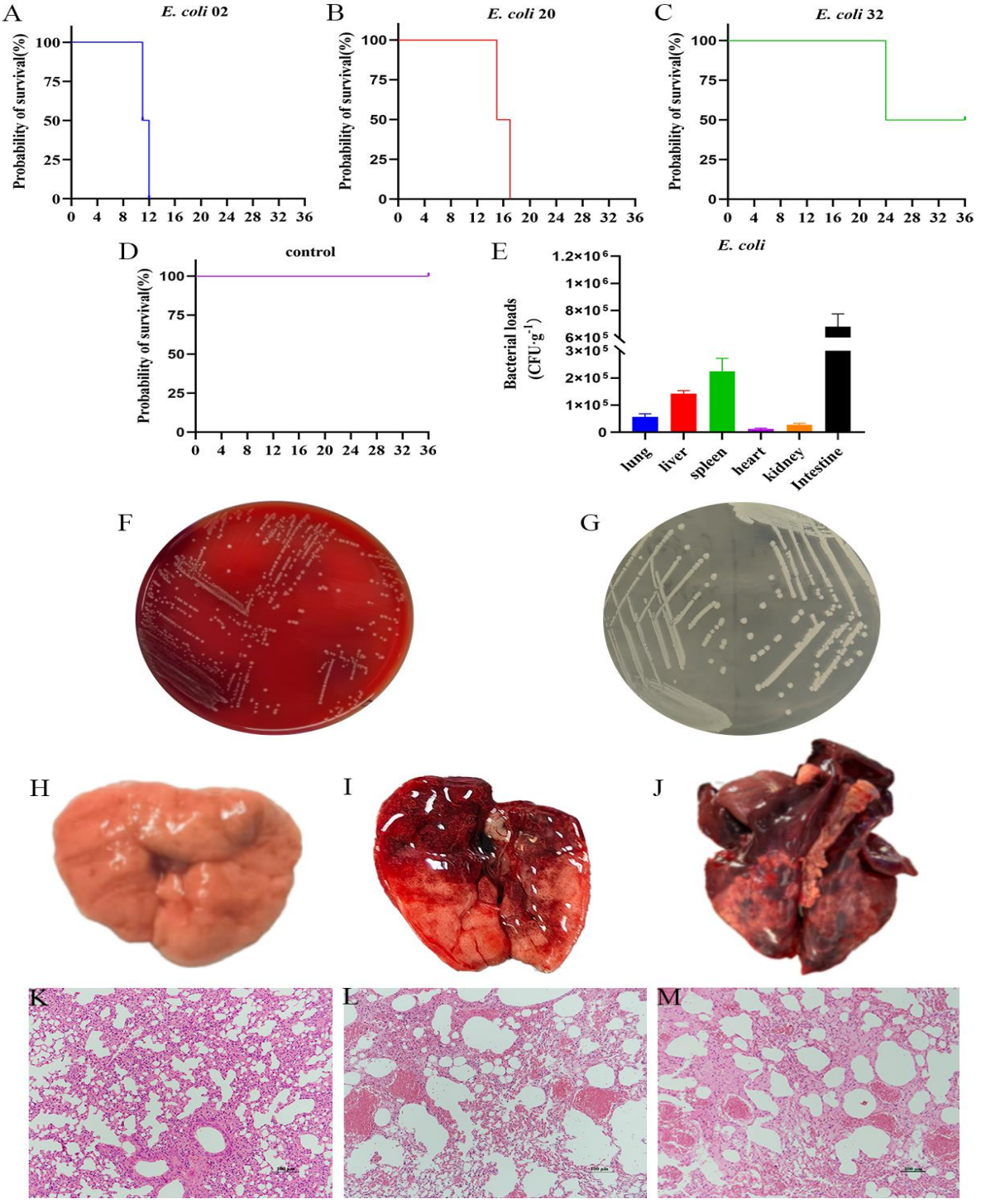


Fig. 6: Pathogenicity of forest musk deer-derived *E. coli* isolates in mice. (A–D) Kaplan–Meier survival curves for mice challenged with *E. coli* 02, *E. coli* 20, *E. coli* 32, and controls. (E) Organ bacterial loads in mice challenged with *E. coli* 32. (F–G) Colony morphology of *E. coli* on blood agar and LB agar plates. (H–J) Gross lungs from a control mouse, an *E. coli* 32-challenged mouse, and a forest musk deer with hemorrhagic pneumonia, respectively. (K–M) Corresponding H&E-stained lung sections (×100).

Table 3: *E. coli* allelic profiles by MLST analysis.

Isolate	MLST loci							ST
	adk	*fumC*	*gyrB*	*icd*	*mdh*	*purA*	*recA*	
E. coli 01	37	38	19	37	17	11	26	95
E. coli 02	37	38	19	37	17	11	26	95
E. coli 03	37	–	19	37	17	11	26	–
E. coli 04	13	40	13	13	23	25	66	357
E. coli 05	6	4	12	1	20	18	7	410
E. coli 06	6	6	5	136	9	7	7	678
E. coli 07	6	29	5	26	24	8	6	937
E. coli 08	6	4	4	16	24	8	121	971
E. coli 09	6	4	12	16	7	5	6	1589
E. coli 10	6	95	3	16	11	8	14	2164
E. coli 11	6	95	3	16	11	8	14	2164
E. coli 12	9	65	5	1	9	13	6	162
E. coli 13	9	65	5	1	9	13	6	162
E. coli 14	9	65	5	1	9	13	6	162
E. coli 15	6	4	33	16	11	8	6	224
E. coli 16	6	4	33	16	11	8	6	224
E. coli 17	6	4	33	16	11	8	6	224
E. coli 18	6	4	33	16	11	8	6	224
E. coli 19	13	40	13	13	23	25	66	357
E. coli 20	13	40	13	13	23	25	66	357
E. coli 21	13	40	13	13	23	25	66	357
E. coli 22	6	95	3	18	11	7	14	1148
E. coli 23	38	38	19	13	17	14	25	–
E. coli 24	80	95	3	18	11	8	333	5869
E. coli 25	6	6	14	21	9	7	7	25
E. coli 26	6	4	12	1	20	8	7	90
E. coli 27	37	38	19	37	17	11	26	95
E. coli 28	37	38	19	37	17	11	26	95
E. coli 29	20	45	41	43	5	32	2	117
E. coli 30	6	4	33	16	11	8	6	224
E. coli 31	6	4	33	16	11	8	6	224
E. coli 32	6	4	33	16	11	8	6	224
E. coli 33	13	40	13	13	23	25	66	357
E. coli 34	13	40	13	13	23	25	66	357
E. coli 35	13	40	13	13	23	25	66	357
E. coli 36	13	40	13	13	23	25	66	357
E. coli 37	6	292	53	140	27	1	2	–
E. coli 38	267	6	5	26	9	13	98	2599
E. coli 39	83	193	530	683	27	–	2	–

Note: "–" indicates an unassigned allele or an allelic profile without an official ST designation.

Similar pulmonary lesions were observed among the three challenge groups. The gross and histological lung images shown in Fig. 6 were obtained from the *E. coli* 32 challenge group. Grossly, lungs from control mice were normal, whereas *E. coli*-challenged mice showed diffuse congestion, swelling, consolidation, and extensive hemorrhage. Similar hemorrhagic necrosis and severe consolidation were observed in forest musk deer that died of hemorrhagic pneumonia (Fig. 6H-J). H&E staining showed normal lung architecture in control mice, whereas *E. coli*-challenged mice exhibited alveolar disruption, septal thickening, inflammatory infiltration, congestion, edema, and focal hemorrhage. The lungs of forest musk deer that died of hemorrhagic pneumonia showed extensive alveolar destruction, interstitial thickening, inflammatory infiltration, congestion, edema, multifocal hemorrhage, and consolidation-like lesions (Fig. 6K-M).

DISCUSSION

As a nationally protected endangered species in China, forest musk deer is important for biodiversity conservation and sustainable musk production. Hemorrhagic pneumonia, characterized by acute onset, rapid progression, and high mortality, is a major constraint on captive forest musk deer breeding. Although several pathogens have been isolated from diseased forest musk deer, the predominant etiological agents and their pathogenic characteristics remain unclear. In this study, *E. coli* was the most frequently isolated bacterium from the lungs of forest musk deer with fatal hemorrhagic pneumonia. The virulence-associated characteristics of the isolates and their pathogenicity in mice supported an association between *E. coli* and pulmonary lesions.

Pulmonary microbial homeostasis is essential for maintaining respiratory health. Previously, healthy lungs were generally considered sterile (Natalini *et al.*, 2023). However, with advances in sequencing technologies, accumulating evidence has revealed that the lungs harbor low-abundance microbial communities maintained in a dynamic equilibrium. Under physiological conditions, these microbial communities contribute to pulmonary homeostasis and play important roles in preventing pathogen invasion and preserving lung tissue integrity. Exposure to increased stocking density, environmental stress, nutritional imbalance, climatic fluctuations, or underlying diseases may disrupt pulmonary microbial homeostasis. Under such conditions, opportunistic pathogens may breach host defense barriers and subsequently colonize and proliferate in lung tissues. Captive forest musk deer are highly sensitive to environmental changes and human disturbances, and their relatively enclosed breeding environments may further predispose them to pulmonary microbial dysbiosis. Once local immune defenses are weakened, opportunistic pathogens originally present at low levels or introduced from external sources may gain a growth advantage, thereby triggering acute inflammatory responses and tissue damage. This pattern of microbial dysbiosis is consistent with microbiome alterations reported in pneumonia and other respiratory diseases (Natalini *et al.*, 2023).

As a typical opportunistic pathogen, *E. coli* is a common member of the intestinal microbiota but can cause extraintestinal infections when host barriers or immune defenses are compromised. In this study, *E. coli* showed substantially higher isolation rates than other bacterial species in the lungs of diseased forest musk deer and was not recovered from animals that died from causes unrelated to hemorrhagic pneumonia. This finding is consistent with previous reports that *E. coli* may be involved in respiratory infections or hemorrhagic pneumonia in ostriches, broiler chickens, goats, dogs, minks, and other animals (Moore *et al.*, 2021; Yu *et al.*, 2021; Kang *et al.*, 2024; Xia *et al.*, 2025), supporting its potential involvement in hemorrhagic pneumonia in forest musk deer. However, metatranscriptomic analysis also detected other respiratory pathogens, and their potential involvement in disease development cannot be excluded. Among the *E. coli* isolates, *fimH* and *fimC* were detected in all isolates, and several isolates also carried virulence-associated genes involved in iron acquisition, serum resistance, tissue invasion, and inflammatory tissue damage. These virulence factors are involved in key pathogenic processes, including adhesion and colonization, iron acquisition, resistance to complement-mediated killing, tissue invasion, and inflammation-mediated tissue damage (Mihailovskaya *et al.*, 2022; Luo *et al.*, 2023; Wei *et al.*, 2024). In particular, *fimH*

contributes to adhesion, invasion, and biofilm formation, whereas *fimC* is required for type I fimbrial assembly, which facilitates bacterial attachment and colonization. These virulence-associated genes may therefore contribute to the ability of the isolates to persist in host tissues and cause damage. The mouse challenge further demonstrated the pathogenic potential of the selected isolates. Moreover, all three challenge isolates exhibited pathogenicity in mice despite substantial differences in their virulence-gene profiles, suggesting that the 12-gene panel alone may not fully account for their in vivo pathogenic potential.

To date, limited information is available regarding the molecular typing of forest musk deer-derived *E. coli*. In this study, the ST composition of lung-derived *E. coli* isolates from deceased forest musk deer was characterized for the first time. In total, 16 assigned STs were identified, including recognized lineages (e.g., ST357, ST224, ST95, ST162, and ST2164), together with 4 unassigned allelic profiles. Several *E. coli* STs can circulate across humans, livestock, poultry, wild animals, and environmental reservoirs and are associated with septicemia, urinary tract infections, avian colibacillosis, and other extraintestinal infections. Among these STs, ST95 is a virulent *E. coli* clonal lineage reported in isolates from humans and animals and associated with extraintestinal infections (Cummins *et al.*, 2022; Adams *et al.*, 2025). ST357 and ST224 are also associated with intestinal infections and septicemia in animals and have been identified among *E. coli* isolates from animal and clinical sources (Nagy *et al.*, 2023). Collectively, the presence of these STs reflects genetic diversity among the forest musk deer-derived *E. coli* isolates, including lineages reported from diverse host and environmental settings (Shimizu *et al.*, 2022; Benlabidi *et al.*, 2023; Jaidane *et al.*, 2025). However, the present findings do not establish the origins of these isolates or the direction of transmission. Future studies should incorporate whole-genome sequencing of isolates from forest musk deer farms, surrounding environments, and contact animals to clarify the transmission pathways of *E. coli* in captive populations.

Antimicrobial resistance represents an important challenge to the prevention and control of hemorrhagic pneumonia in forest musk deer. Under captive breeding conditions, antimicrobial agents are frequently used to treat and prevent respiratory diseases. However, long-term, repeated, or empirical antimicrobial use may impose selective pressure and promote the emergence and dissemination of resistant strains. In this study, the forest musk deer-derived *E. coli* isolates exhibited resistance to multiple commonly used antimicrobial agents, and more than 50% of the isolates were MDR. Similar resistance phenotypes have previously been reported in forest musk deer-derived *E. coli*, including resistance to Kanamycin, GEN, and AMP (Luo *et al.*, 2016), and comparable resistance patterns have also been observed in isolates from Shaanxi Province (Yang *et al.*, 2025). For rare and endangered species such as forest musk deer, infections caused by antimicrobial-resistant bacteria may compromise treatment efficacy, restrict therapeutic options, and increase the risk of prolonged disease and mortality. Therefore, the prevention and control of hemorrhagic pneumonia in forest musk deer should not rely solely on empirical antimicrobial therapy. Instead, targeted treatment strategies based on pathogen isolation, antimicrobial susceptibility testing, and regular resistance surveillance should be implemented. Specifically, commonly used antimicrobial classes, including β-lactams, fluoroquinolones, and aminoglycosides, should be selected according to breeding farm-specific resistance profiles and surveillance data. Such an approach may help reduce inappropriate or prolonged antimicrobial use and mitigate antimicrobial selection pressure. Strengthened isolation measures and epidemiological source tracing should be implemented to limit the dissemination of isolates resistant to multiple antimicrobial agents within forest musk deer populations and breeding environments. Future studies incorporating whole-genome sequencing should comprehensively characterize antimicrobial resistance genes, plasmids, integrons, pathogenicity islands, other mobile genetic elements, and additional virulence determinants, and examine their associations with specific STs (Leekitcharoenphon *et al.*, 2021). Such studies would provide further insight into the molecular mechanisms of antimicrobial resistance and virulence in forest musk deer-derived *E. coli*.

Conclusions: In summary, *E. coli* was frequently isolated from fatal hemorrhagic pneumonia cases in forest musk deer. The isolates exhibited antimicrobial resistance, virulence-associated gene carriage, and pathogenic potential in mice, supporting a possible role in disease development. This study provides the first characterization of the MLST diversity of lung-derived *E. coli* isolates from dead forest musk deer, identifying 16 assigned STs, including ST95, ST357, and ST224, and 4 unassigned allelic profiles. These findings provide a basis for pathogen surveillance, antimicrobial susceptibility-guided treatment, and targeted prevention and control of hemorrhagic pneumonia in captive forest musk deer.

Limitations: This study has several limitations. First, because forest musk deer is a rare and endangered species, lung tissues from clinically healthy animals could not be obtained as controls for ethical reasons, and all available lung samples were collected from deceased animals. Although prompt aseptic sampling was performed and *E. coli* was not isolated from lung samples from animals that died from causes unrelated to hemorrhagic pneumonia, the possibility of postmortem translocation of *E. coli* cannot be completely excluded. Second, metatranscriptomic sequencing was performed on only three of the 43 lung samples as an exploratory analysis of the pulmonary microbial community, and these findings may not fully represent the microbial diversity of the entire case series. Third, pathogenicity was evaluated only in a mouse model because infection experiments could not be performed in forest musk deer. The high-dose intraperitoneal inoculation used in this model does not fully reproduce natural respiratory infection. Therefore, the mouse model can only partially reflect the pathogenic potential and pulmonary tissue-damaging capacity of forest musk deer-derived *E. coli* isolates, and their direct pathogenic role in hemorrhagic pneumonia remains to be further established. Fourth, whole-genome sequencing was not performed on the *E. coli* isolates obtained in this

study. Antimicrobial resistance genes, plasmids, pathogenicity islands, mobile genetic elements, and additional virulence determinants could not be comprehensively characterized.

Authors Contributions: Conceptualization: CL, LZ, KG; Methodology: CL, LZ, KG; Investigation: WL, YJ, YY, ZM, RY, XZ, WD, FY, SF; Data Curation: YF, LYZ; Writing–Original Draft: WD, FY, SF, MT; Writing–Review & Editing: LZ, KG.

Acknowledgments: We would like to thank Editage (www.editage.cn) for English language editing.

Generative AI Statement: During the preparation of this manuscript, the authors used ChatGPT for language editing. The authors subsequently reviewed and edited the content as necessary and assume full responsibility for the accuracy and integrity of the published work.

Funding: This work was supported by the Research project on pathogenesis and prevention and control technology of forest musk deer in Fengxian County in 2023 [Project No. JXBJ-DL-(2023-1005)], the Research and Application of Prevention and Treatment Technology of Respiratory Diseases in Captive Forest Musk Deer [Project No. S2023-YF-YBNY-0528], and the Screening of Plant Anti-inflammatory Components and Their Application in Livestock and Poultry Feed Additives [Project No. BSKYQD-18].

Ethics Statement: All animal experiments were approved by the Executive Ethics Committee of Laboratory Animal Management and Ethics Inspection of Northwest A&F University, Xianyang, China (IACUC2023–0703). This study is reported in accordance with the Animal Research: Reporting of In Vivo Experiments (ARRIVE) 2.0 guidelines.

Availability of data and material: Data generated or analyzed during this study are available from the corresponding author on reasonable request.

Conflicts of interest: The authors declare no conflict of interest.

REFERENCES

Adams JRG, Long H, Birdsall CA, *et al.*, 2025. High-risk clonal groups of avian pathogenic *Escherichia coli* (APEC) demonstrate heterogeneous phenotypic characteristics in vitro and in vivo. Virulence 16(1):2546682.

Benlabidi S, Raddaoui A, Lengliz S, *et al.*, 2023. Occurrence of high-risk clonal lineages ST58, ST69, ST224, and ST410 among extended-spectrum β-lactamase-producing *Escherichia coli* isolated from healthy free-range chickens (*Gallus gallus domesticus*) in a rural region in Tunisia. Genes 14(4):875.

Chen Q, Zhao K, Li H, *et al.*, 2022. Antibacterial and anti-virulence effects of furazolidone on *Trueperella pyogenes* and *Pseudomonas aeruginosa*. BMC Veterinary Research 18(1):114.

Clinical and Laboratory Standards Institute (CLSI), 2023. Performance Standards for Antimicrobial Susceptibility Testing. 33rd ed. CLSI supplement M100. Clinical and Laboratory Standards Institute, USA.

Coe SE, Magagna MA, Zimmerman A, *et al.*, 2022. Extraintestinal pathogenic *Escherichia coli* causes necrohemorrhagic pneumonia in multiple research dogs. Toxicologic Pathology 50(8):904-909.

Cummins ML, Reid CJ and Djordjevic SP, 2022. F plasmid lineages in *Escherichia coli* ST95: Implications for host range, antibiotic resistance, and zoonoses. mSystems 7(1):e01212-21.

Deng Y, Wang Y, Liu Y, *et al.*, 2025. *Akkermansia muciniphila* isolated from forest musk deer ameliorates diarrhea in mice via modification of gut microbiota. Animal Models and Experimental Medicine 8(2):295-306.

Fan J, Zheng X, Wang H, *et al.*, 2019. Analysis of genetic diversity and population structure in three forest musk deer captive populations with different origins. G3: Genes, Genomes, Genetics 9(4):1037-1044.

Huang T, Zhang M, Tong X, *et al.*, 2019. Microbial communities in swine lungs and their association with lung lesions. Microbial Biotechnology 12(2):289-304.

Iorgoni V, Iancu I, Popa I, *et al.*, 2025. First report of respiratory infection caused by multidrug-resistant *Escherichia coli* in an ostrich in Romania. Antibiotics 14(4):354.

Jaidane N, Naas T, Boughattas S, *et al.*, 2025. Occurrence of *mcr-1.1*-producing *Escherichia coli* in clinical settings in Tunisia. Journal of Global Antimicrobial Resistance 44:149-151.

Jiang Y, Han X, Li M, *et al.*, 2022. Changes in the gut microbiota of forest musk deer (*Moschus berezovskii*) during ex situ conservation. Frontiers in Microbiology 13:969593.

Kang D, Womble M, Cullen JM, *et al.*, 2024. Severe bronchiectasis resulting from chronic bacterial bronchitis and bronchopneumonia in a jungle cat. Journal of Veterinary Diagnostic Investigation 36(1):131-136.

Kobayashi T, Ikeda M, Okada Y, *et al.*, 2021. Clinical and microbiological characteristics of recurrent *Escherichia coli* bacteremia. Microbiology Spectrum 9(3):e01399-21.

Leekitcharoenphon P, Johansson MHK, Munk P, *et al.*, 2021. Genomic evolution of antimicrobial resistance in *Escherichia coli*. Scientific Reports 11(1):15108.

Liu C, Hong T, Yu L, *et al.*, 2024. Single-nucleus multiomics unravels the genetic mechanisms underlying musk secretion in Chinese forest musk deer (*Moschus berezovskii*). International Journal of Biological Macromolecules 279:135050.

Lu B, Yao X, Han G, *et al.*, 2022. Isolation of *Klebsiella pneumoniae* phage vB_KpnS_MK54 and pathological assessment of endolysin in the treatment of pneumonia mice model. Frontiers in Microbiology 13:854908.

Lubkin A, Bernard-Raichon L, DuMont AL, *et al.*, 2024. SARS-CoV-2 infection predisposes patients to coinfection with *Staphylococcus aureus*. mBio 15(8):e01667-24.

Luo S, Liao C, Peng J, *et al.*, 2023. Resistance and virulence gene analysis and molecular typing of *Escherichia coli* from duck farms in Zhanjiang, China. Frontiers in Cellular and Infection Microbiology 13:1202013.

Luo X, Wang P, Cheng JG, *et al.*, 2016. Characterization of virulence genes and antimicrobial resistance of lung pathogenic *Escherichia coli* isolates in forest musk deer (*Moschus berezovskii*). Journal of Zoo and Wildlife Medicine 47(2):540-550.

Miao Y, Zhao X, Lei J, *et al.*, 2023. Characterization of lung microbiomes in pneumonic Hu sheep using culture technique and *16S rRNA* gene sequencing. Animals 13(17):2763.

Mihailovskaya VS, Remezovskaya NB, Zhdanova IN, *et al.*, 2022. Virulence potential of faecal *Escherichia coli* strains isolated from healthy cows and calves on farms in Perm Krai. Vavilov Journal of Genetics and Breeding 26(5):486-494.

Moore MEG, Paulin-Curlee G, Johnston BD, *et al.*, 2021. Molecular characteristics, ecology, and zoonotic potential of *Escherichia coli* strains that cause hemorrhagic pneumonia in animals. Applied and Environmental Microbiology 87(23):e01471-21.

Nagy JB, Koleszár B, Khayer B, *et al.*, 2023. Carbapenem-resistant *Escherichia coli* in black-headed gulls, the Danube, and human clinical samples: A One Health comparison of contemporary isolates. Journal of Global Antimicrobial Resistance 35:257-261.

Natalini JG, Singh S and Segal LN, 2023. The dynamic lung microbiome in health and disease. Nature Reviews Microbiology 21(4):222-235.

Qi WH, Hu LF, Gu YJ, *et al.*, 2024. Integrated mRNA-miRNA transcriptome profiling of blood immune responses potentially related to pulmonary fibrosis in forest musk deer. Frontiers in Immunology 15:1404108.

Shimizu T, Kido N, Miyashita N, *et al.*, 2022. Antimicrobial resistance in *Escherichia coli* isolates from Japanese raccoon dogs (*Nyctereutes viverrinus*) in Kanagawa Prefecture, Japan: Emergence of extended-spectrum cephalosporin-resistant human-related clones. Journal of

Medical Microbiology 71(12):001631.

Wan SH, Li N, Zheng P, *et al.*, 2025. Virulence characteristics and antibiotic resistance analysis of *Klebsiella pneumoniae* isolated from pig farms in Xinjiang, China: revealing potential zoonotic risks. Porcine Health Management 11(1):25.

Wang Z, Lu G, Gao Y, *et al.*, 2023. mtDNA CR evidence indicates high genetic diversity of captive forest musk deer in Shaanxi Province, China. Animals 13(13):2191.

Wei S, Ding B, Wang G, *et al.*, 2024. Population characteristics of pathogenic *Escherichia coli* in puerperal metritis of dairy cows in Ningxia region of China: a systemic taxa distribution of virulence factors and drug resistance genes. Frontiers in Microbiology 15:1364373.

Xia Z, Luo G, Gou LY, *et al.*, 2025. Metaviromic and metagenomic study of the pathogens in unexplained pneumonia cases in goats. Veterinary Microbiology 304:110469.

Yang K, Wu X, Ding H, *et al.*, 2025. Isolation, identification, and antibiotic resistance, CRISPR system analysis of *Escherichia coli* from forest musk deer in Western China. Microorganisms 13(7):1683.

Yang W, Wang WY, Zhao W, *et al.*, 2020. Preliminary study on the role of novel LysR family gene *kp05372* in *Klebsiella pneumoniae* of forest musk deer. Journal of Zhejiang University-SCIENCE B 21(2):137-154.

Yehia N, Salem HM, Mahmmod Y, *et al.*, 2023. Common viral and bacterial avian respiratory infections: an updated review. Poultry Science 102(5):102553.

Yi L, Jiang H, Li Y, *et al.*, 2025. Hair metabolomic profiling of diseased forest musk deer (*Moschus berezovskii*) using ultra-high-performance liquid chromatography-tandem mass spectrometry (UHPLC-MS/MS). Animals 15(14):2155.

Yu Y, Hu B, Fan H, *et al.*, 2021. Molecular epidemiology of extraintestinal pathogenic *Escherichia coli* causing hemorrhagic pneumonia in mink in northern China. Frontiers in Cellular and Infection Microbiology 11:781068.

Yun J, Mao L, Li J, *et al.*, 2022. Molecular characterization and antimicrobial resistance profile of pathogenic *Escherichia coli* from goats with respiratory disease in eastern China. Microbial Pathogenesis 166:105501.

Zhang Y, Wang R, Hu Q, *et al.*, 2024. Characterization of *Pseudomonas aeruginosa* bacteriophages and control hemorrhagic pneumonia on a mice model. Frontiers in Microbiology 15:1396774.

Zhao W, Tian Q, Luo Y, *et al.*, 2017. Isolation, identification, and genome analysis of lung pathogenic *Klebsiella pneumoniae* (LPKP) in forest musk deer (*Moschus berezovskii*). Journal of Zoo and Wildlife Medicine 48(4):1039-1048.

Zhao W, Yu D, Cheng J, *et al.*, 2020. Identification and pathogenicity analysis of *Streptococcus equinus* FMD1, a beta-hemolytic strain isolated from forest musk deer lung. Journal of Veterinary Medical Science 82(2):172-176.

Zhou Y, Shao Z, Dai G, *et al.*, 2023. Pathogenic infection characteristics and risk factors for bovine respiratory disease complex based on the detection of lung pathogens in dead cattle in Northeast China. Journal of Dairy Science 106(1):589-606.